Mutations of optineurin in amyotrophic lateral sclerosis

Hirofumi Maruyama[1], Hiroyuki Morino[1], Hidefumi Ito[2]†, Yuishin Izumi[3], Hidemasa Kato[4], Yasuhito Watanabe[5], Yoshimi Kinoshita[2], Masaki Kamada[1,3], Hiroyuki Nodera[3], Hidenori Suzuki[6], Osamu Komure[7], Shinya Matsuura[8], Keitaro Kobatake[9], Nobutoshi Morimoto[10], Koji Abe[10], Naoki Suzuki[11], Masashi Aoki[11], Akihiro Kawata[12], Takeshi Hirai[12], Takeo Kato[13], Kazumasa Ogasawara[14], Asao Hirano[15], Toru Takumi[5], Hirofumi Kusaka[2], Koichi Hagiwara[16], Ryuji Kaji[3] & Hideshi Kawakami[1]

Amyotrophic lateral sclerosis (ALS) has its onset in middle age and is a progressive disorder characterized by degeneration of motor neurons of the primary motor cortex, brainstem and spinal cord[1]. Most cases of ALS are sporadic, but about 10% are familial. Genes known to cause classic familial ALS (FALS) are superoxide dismutase 1 (*SOD1*)[2], *ANG* encoding angiogenin[3], *TARDP* encoding transactive response (TAR) DNA-binding protein TDP-43 (ref. 4) and fused in sarcoma/translated in liposarcoma (*FUS*, also known as *TLS*)[5,6]. However, these genetic defects occur in only about 20–30% of cases of FALS, and most genes causing FALS are unknown. Here we show that there are mutations in the gene encoding optineurin (*OPTN*), earlier reported to be a causative gene of primary open-angle glaucoma (POAG)[7], in patients with ALS. We found three types of mutation of *OPTN*: a homozygous deletion of exon 5, a homozygous Q398X nonsense mutation and a heterozygous E478G missense mutation within its ubiquitin-binding domain. Analysis of cell transfection showed that the nonsense and missense mutations of *OPTN* abolished the inhibition of activation of nuclear factor kappa B (NF-κB), and the E478G mutation revealed a cytoplasmic distribution different from that of the wild type or a POAG mutation. A case with the E478G mutation showed OPTN-immunoreactive cytoplasmic inclusions. Furthermore, TDP-43- or SOD1-positive inclusions of sporadic and *SOD1* cases of ALS were also noticeably immunolabelled by anti-OPTN antibodies. Our findings strongly suggest that OPTN is involved in the pathogenesis of ALS. They also indicate that NF-κB inhibitors could be used to treat ALS and that transgenic mice bearing various mutations of *OPTN* will be relevant in developing new drugs for this disorder.

We analysed six Japanese individuals from consanguineous marriages who had ALS; two of them were siblings, the others were from independent families. We used homozygosity mapping, which has been shown to identify a locus of a disease-causing gene from as few as three individuals[8]. We performed a genome-wide scan of single nucleotide polymorphisms (SNPs) by using the GeneChip Human Mapping 500K Array Set (Affymetrix), and selected for the run of homozygous SNPs (RHSs) more than 3 centimorgans in length. Under this condition, the RHSs are able to retrieve more than 98% of the entire length of the autozygous segments created as a result of a first-cousin or second-cousin marriage (Supplementary Information)[8]. We extracted RHSs of six individuals (Supplementary Fig. 1a). A region (hg18: 12,644,480–15,110,539) in chromosome 10, which was an overlap among four subjects, was chosen as the primary candidate region (Supplementary Fig. 1b). Assuming that subjects ii, iii, v and vi had the same disease gene, the chance that the overlap had the disease gene was $P_{ii+iii+v+vi} = 0.935$ (Supplementary Information). We listed up to 17 candidate genes in the region and sequenced their exons (Supplementary Fig. 1c). We detected a deletion of exon 5 in the *OPTN* (also known as FIP-2 (ref. 9)) gene in two siblings (Fig. 1a, family 1, subjects 1 and 2). PCR with a forward primer of exon 4 and a reverse primer of intron 5 revealed a 2.5-kilobase (kb) band in the control, V-3 and IV-1, and a 0.7-kb band in IV-1, subject 1 and subject 2 (Fig. 1b). Direct sequence analysis of the short band showed the joining of the 5′ part of AluJb in intron 4 and the 3′ part of AluSx in intron 5 with 12-base-pair (bp) microhomology (Fig. 1c). Thus, the deletion resulted from Alu-mediated recombination. We also found a homozygous nonsense c.1502C>T mutation (Q398X, exon 12) in the gene in one individual with ALS (Fig. 1d, e, family 2, subject 3). For the other three subjects, we found neither mutations nor copy number changes in the *OPTN* gene, although we did not completely exclude the possibility of mutations in introns or intergenic regions in the gene. We extended our analysis of *OPTN* to ten additional individuals from consanguineous marriages who had ALS, 76 individuals with familial ALS and 597 individuals with sporadic ALS (SALS). We found the Q398X mutation in a sporadic individual (subject 4, family 3; Fig. 1d). Subjects 3 and 4, who were not related according to their family history, shared their haplotype for a 0.9-megabase (Mb) region (hg18: chr10: 12,973,261–13,879,735) containing the *OPTN* gene (Supplementary Table 1). We investigated a total of 170 copies of chromosome 10 from 85 Japanese subjects genotyped for the HapMap3 project, and found that the incidental length of haplotype sharing around *OPTN* gene was at most 320 kb. Given that a haplotype sharing of 0.9 Mb rarely occurs by chance, the mutation is likely to have been derived from a single ancestor (Supplementary Fig. 1d). Subjects 1 and 2 shared their haplotype for an 8.3-Mb

[1]Department of Epidemiology, Research Institute for Radiation Biology and Medicine, Hiroshima University, Hiroshima 734-8553, Japan. [2]Department of Neurology, Kansai Medical University, Moriguchi 570-8506, Japan. [3]Department of Clinical Neuroscience, University of Tokushima Graduate School, Tokushima 770-8503, Japan. [4]Division of Developmental Biology, Research Center for Genomic Medicine, Saitama Medical University, Saitama 350-1241, Japan. [5]Laboratory of Integrative Bioscience, Hiroshima University Graduate School of Biomedical Sciences, Hiroshima 734-8553, Japan. [6]Faculty of Human Science, Hiroshima Bunkyo Women's University, Hiroshima 731-0295, Japan. [7]South Osaka Neurosurgical Hospital, Osakasayama 589-0011, Japan. [8]Department of Genetics and Cell Biology, Research Institute for Radiation Biology and Medicine, Hiroshima University, Hiroshima 734-8553, Japan. [9]Department of Neurology, Kobatake Hospital, Fukuyama 720-1142, Japan. [10]Department of Neurology, Okayama University, Graduate School of Medicine, Dentistry, and Pharmaceutical Sciences, Okayama 700-8558, Japan. [11]Department of Neurology, Tohoku University School of Medicine, Sendai 980-8574, Japan. [12]Department of Neurology, Tokyo Metropolitan Neurological Hospital, Fuchu, Tokyo 183-0042, Japan. [13]Department of Neurology, Haematology, Metabolism, Endocrinology and Diabetology, Yamagata University Faculty of Medicine, Yamagata 990-9585, Japan. [14]Department of Pathology, School of Medicine, Shiga University of Medical Science, Ohtsu 520-2192, Japan. [15]Division of Neuropathology, Department of Pathology, Montefiore Medical Center, New York, New York 10467-2490, USA. [16]Department of Respiratory Medicine, Saitama Medical University, Saitama 350-0495, Japan. †Present address: Department of Neurology, Kyoto University Graduate School of Medicine, Kyoto 606-8507, Japan.

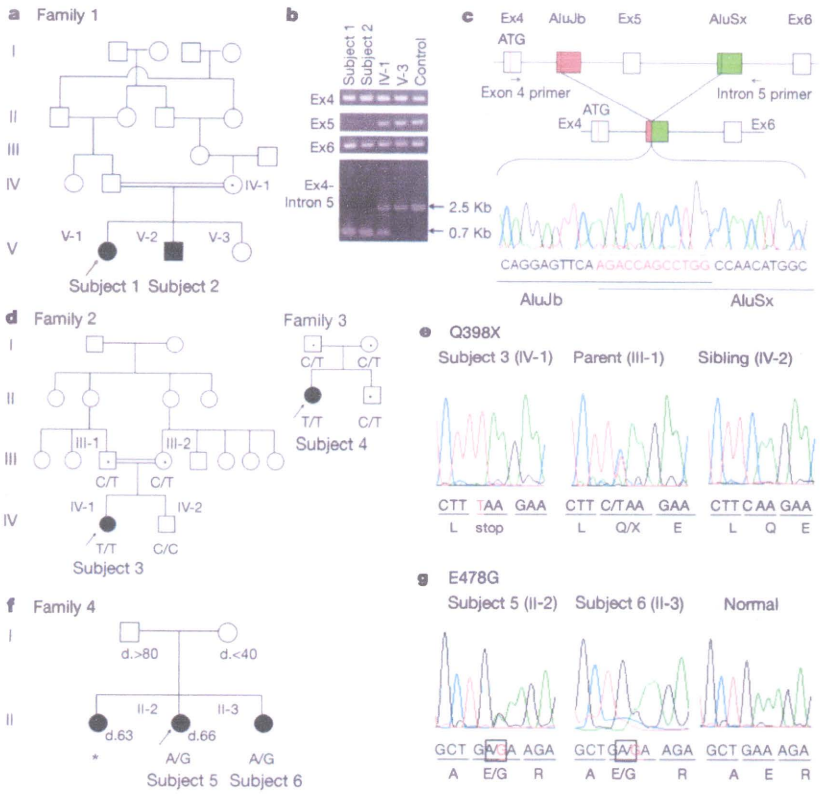

Figure 1 | Exon 5 deletion, nonsense and missense mutations of the *OPTN* gene. **a**, Family 1. The filled circle or square indicate the affected individuals; the arrows indicate the probands. **b**, Agarose gel electrophoretogram. Subject 1 (V-1) and subject 2 (V-2) showed lack of exon 5 PCR product and shortened product of exon 4 to intron 5. **c**, Chromatogram with OPTN deletion of exon 5 and schematic structure of deleted gene. **d**, Families 2 and 3. Dots indicate heterozygous carriers. **e**, Chromatograms from index subjects with OPTN mutation of c.1502 C>T. Homozygous mutation is in red, and the mutation is indicated by using the single-letter amino-acid code. **f**, Family 4. *DNA sample could not be obtained. Numerals show the age at death. **g**, Chromatograms from index subjects with the OPTN mutation of c.1743A>G. The heterozygous mutation is marked by the square.

region (hg18: chr10: 6,815,934–14,842,351), which contained the *OPTN* gene and was different from that in subjects 3 and 4 (Supplementary Table 1).

In the screening of ALS families, we identified a heterozygous missense mutation (c1743A>G, E478G, exon14, Fig. 1g) of *OPTN* in four individuals with ALS in two families with ALS. Subjects 5 and 6 were sisters, and the pedigree suggests that the mutation had an autosomal dominant trait with incomplete penetrance (Fig. 1f, family 4). Subjects 7 and 8 (family 5) were brothers. Although these families are not related according to their family history, subjects 5–8 shared their haplotype for 2.3 Mb (hg18: chr10: 11,460,985–13,703,017, Supplementary Table 3), again suggesting that the mutation was derived from a single ancestor. Indeed, the Q398X nonsense and E478G missense mutations were not observed in 781 healthy Japanese volunteers as well as in over 6,800 (including 1,728 Japanese) individuals in the glaucoma studies, where the entire coding region of the gene was investigated (Supplementary Table 2). Collectively, the mutation was absent over a total of 5,000 Japanese chromosomes. The deletion mutation was also absent in 200 Japanese, and not reported in the over 6,800 glaucoma individuals. The co-segregation of three different mutations of *OPTN* with the ALS phenotype strongly suggests that some mutations of *OPTN* cause ALS.

The eight individuals with mutations of *OPTN* showed onset from 30 to 60 years of age. Most of them showed a relatively slow progression and long duration before respiratory failure, although the clinical phenotypes were not homogeneous (see Supplementary Information).

The Q398X mutation causes a premature stop during translation, truncating the 577 amino-acid OPTN protein to one of 397 amino acids in length. This truncation results in a deletion of the coiled coil 2 domain[10], which is necessary for binding to ubiquitin[11], huntingtin[12] (htt), myosin VI[13] and the ubiquitinated receptor-interacting protein[14]. In the gene with the deletion of exon 5, if there was a transcript, the transcript splicing from exon 4 to exon 6 would cause a frame shift and make a stop codon (TGA in the ninth to eleventh codons in exon 6), which would be expected to translate a peptide 58 amino acids in length. The missense mutation (E478G) was located between coiled coil 2 domain and the leucine zipper domain. This glutamic acid is highly conserved among OPTN proteins of a wide range of species (Supplementary Fig. 2a), and is situated within the DFxxER motif, an ubiquitin-binding domain shared among OPTN, NF-κB essential molecule (NEMO), and A20 binding and inhibitor of NF-κB proteins (ABIN) (Supplementary Fig. 2b). The mutations in the DFxxER motif in ABIN reduce the binding to ubiquitin, which render them unable to inhibit NF-κB activation[11]. We investigated the ability of various mutations of *OPTN* to inhibit NF-κB-mediated transcriptional activation by performing a luciferase assay using NSC-34 cells (a mouse neuroblastoma and spinal-cord hybrid cell line) transfected with wild-type or mutant *OPTN*. E50K *OPTN*, which causes POAG[7], downregulated the NF-κB activity, as did the wild type. On the other hand, both Q398X and E478G had no ability to inhibit NF-κB activity (Tukey–Kramer, $P < 0.05$). These tendencies were retained after stimulation with tumour-necrosis factor (TNF)-α (Fig. 2A). We also examined the subcellular localization of overexpressed Flag-tagged wild-type OPTN (wild type) and its mutants in cells (Fig. 2B). Immunofluorescence staining was performed with their antibodies against Flag and the Golgi matrix marker GM130. Confocal images showed close apposition of granular signals of wild-type OPTN or E50K with GM130 (see g and i in Fig. 2B)[15,16]. E50K often shapes large granular structures near the Golgi apparatus. E478G rarely showed granular signals (see b in Fig. 2B); however, when closely observed, some of the signals were still closely localized to GM130 (see h in Fig. 2B). Western blotting using a lysate of transformed lymphoblasts showed that the 74-kDa band, corresponding to OPTN, was absent in subjects 3 and 4, but was present in the non-diseased mother and brother of subject 3 (Supplementary Fig. 3a). Quantitative PCR with reverse transcription

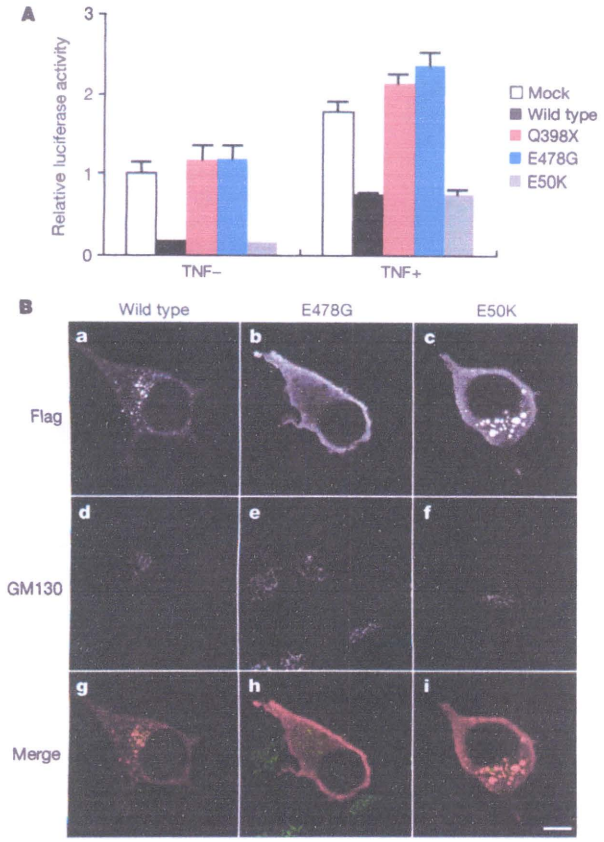

Figure 2 | Influence of OPTN mutations. A, Luciferase assay to assess the ability of various OPTNs to inhibit activation of NF-κB. The wild type and E50K have a similar NF-κB activation-inhibiting effect, whereas mock, Q398X and E478G types lack this effect. Error bars, standard deviations of triplicate assays. **B,** Localization of OPTN. Flag is the white signals in a–c and red signals in g–i. GM130 is the white signals in d–f and green signals in g–i. The wild type shows many fluorescent granules closely localized with the Golgi apparatus. E478G OPTN shows a reduced number of granules, and rarely co-localized with the Golgi apparatus. E50K OPTN granules have become large and closely localized with the Golgi apparatus. Scale bar, 10 μm.

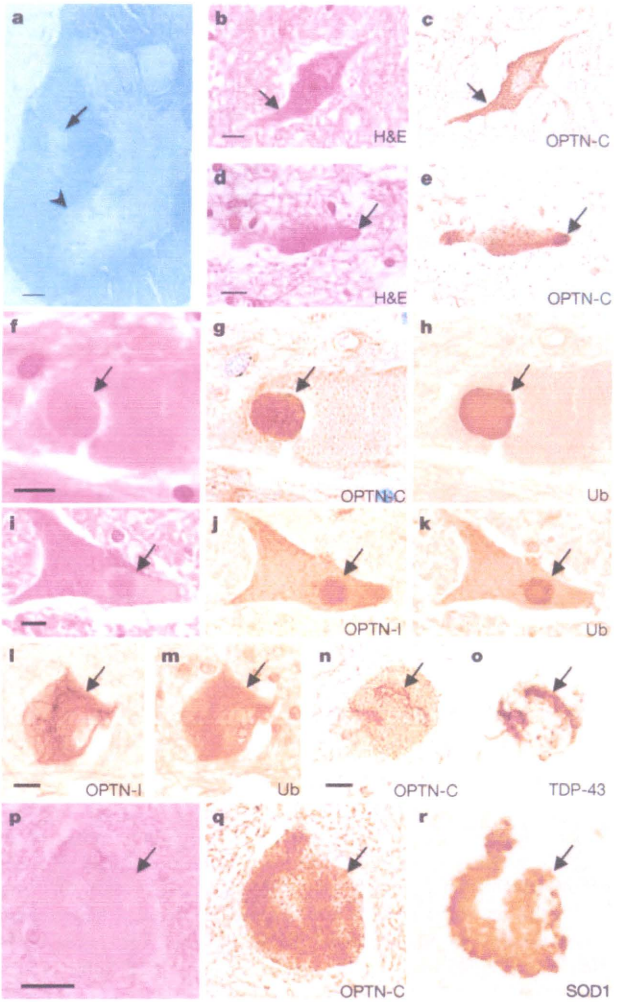

Figure 3 | Identification of OPTN in distinctive intracytoplasmic inclusions of subjects with ALS. a–e, Neuropathology of the lumbar spinal cord from subject 5. Klüver-Barrera (**a**) show loss of myelin from the corticospinal tract (arrow) and loss of motor neurons from the anterior horn (arrowhead). The cytoplasm of the remaining motor neurons contains an amorphous eosinophilic region (**b**, arrow). H&E, haematoxylin and eosin. The same neuron was re-stained with the anti-OPTN antibody (**c**, arrow). The eosinophilic retention occasionally appears to form a hyaline inclusion (**d**, arrow), which is intensely immunolabelled with the anti-OPTN antibody (**e**, arrow). **f–k,** Round hyaline inclusions of subjects with SALS (**f**, **i**) are immunolabelled with anti-OPTN-C and anti-OPTN-I antibodies (**g** and **j**, respectively). The sections were re-stained with anti-ubiquitin (Ub) antibodies (**h**, **k**). **l–o,** Skein-like inclusions of patients with SALS are reactive with the anti-OPTN-I and anti-OPTN-C antibodies (**l**, **n**). Re-staining of **l** with the anti-ubiquitin antibody (**m**) and **n** with anti-TDP-43 antibody (**o**). **p–r,** Lewy-body-like hyaline inclusion of a patient with FALS, stained with haematoxylin and eosin (**p**), anti-OPTN-C antibody (**q**) and SOD1 antibody (**r**). Scale bars, 200 μm (**a**), 20 μm (**b–p**).

revealed that the products were diminished to 58.0% in the heterozygote (III-2) and to 13.8% in the homozygote (subject 4) compared with the control levels (Supplementary Fig. 3b). In addition, cycloheximide recovered the decrease in the OPTN messenger RNA (mRNA) with the mutation (Supplementary Fig. 3c). Thus mRNA with this mutation, which bears a premature termination, might be degraded through nonsense-mediated mRNA decay in lymphoblasts.

The spinal cord from subject 5 with the E478G mutation revealed loss of myelin from the corticospinal tract and of the anterior horn cells (AHCs, Fig. 3a and Supplementary Fig. 4a, b). OPTN immunohistochemistry demonstrated increased staining intensity of the cytoplasm of the remaining AHCs and the neurites in the anterior horn (Supplementary Fig. 4c). Higher magnification of the motor neurons revealed intracytoplasmic eosinophilic inclusions (Fig. 3b, d). Intriguingly, these inclusions were distinctly immunopositive for OPTN (Fig. 3c, e). On the other hand, the cytoplasm of AHCs from control individuals was faintly labelled with anti-OPTN antibodies (Supplementary Fig. 5a, c), similar to the spinal-cord AHCs of mice (Supplementary Fig. 6b) and in contrast to the highly labelled sensory neurons in the dorsal root ganglia of mice (Supplementary Fig. 6d). In patients with sporadic ALS, the staining intensity for OPTN apparently increased not only in the cytoplasm of the remaining AHCs but also in their neurites (Supplementary Fig. 5b, d). In addition, distinctive intracytoplasmic inclusions were also noticeably OPTN immunolabelled in cases of sporadic and familial ALS; eosinophilic round hyaline inclusions from patients with SALS were immunopositive for OPTN (Fig. 3f, g, i, j). Re-staining of the same sections for ubiquitin, a known constituent of many neurodegenerative inclusions, revealed that these inclusions were also positive and faithfully matched the distribution of OPTN immunoreactivity (Fig. 3h, k). The anti-OPTN antibodies also stained skein-like inclusions (Fig. 3l, n), which were again mirrored with the anti-ubiquitin antibodies (Fig. 3m) and with the anti-TDP-43

antibodies (Fig. 3o). The distinct OPTN immunoreactivity of ubiquitin- and TDP-43-positive intracytoplasmic inclusions was confirmed on serial sections from patients with SALS (Supplementary Fig. 7). Moreover, SOD1-immunopositive Lewy-body-like hyaline inclusions from cases with *SOD1* FALS were also immunopositive for OPTN (Fig. 3p–r). We found that OPTN antibody labelled both SOD1- and TDP-43-positive inclusions. As the staining of SOD1 and TDP-43 is generally mutually exclusive, OPTN staining appears to be a more general marker for inclusions in various types of ALS; therefore, the OPTN molecule might also be involved in a broader pathogenesis of ALS.

The mutations of the *OPTN* gene cause both recessive and dominant traits, and the mechanism causing the disease may be different between the two traits. The Q398X nonsense mutation and probably the exon 5 deletion mutation cause a decrease in OPTN expression resulting from nonsense-mediated mRNA decay of the transcript carrying the nonsense OPTN mutations. Therefore, the mutated OPTN protein by itself is unlikely to disturb cell function or to be included in the inclusion body in the motor neuron cells. The mechanism of recessive mutations causing ALS is expected to be simply loss of function, and the heterozygote for the Q398X mutation does not develop the ALS phenotype. On the other hand, the E478G missense mutation increased the immunoreactivity for OPTN in the cell body and the neurites. The increased amount and different distribution of the mutated protein would disturb neuronal functions, and may accelerate the inclusion body formation as well as the increase and the different distribution of OPTN immunoreactivity in sporadic ALS. Thus the heterozygote for the E478G mutation will develop the disease.

The different impact on NF-κB signalling and the different intracellular localization of ALS- and POAG-linked mutated protein may explain the phenotypic divergence between the two diseases. Subject 3 with homozygotic Q398X also showed POAG, whereas subject 4 with the same mutation, and subjects 1 and 2 with the exon 5 deletion, did not show it. The prevalence of POAG in the population older than 40 years is 3.9% in Japan[17].Considering this information, the ALS and glaucoma in subject 3 may accidentally coexist.

OPTN competes with NEMO for binding to the ubiquitinated receptor-interacting protein and negatively regulates TNF-α-induced activation of NF-κB[14], which mediates an upregulation of OPTN, creating a negative feedback loop[18]. ALS-related OPTN mutations lacked the inhibitory effect towards NEMO, and thus exaggerated NF-κB activation. In sporadic ALS, a previous report showed that NF-κB, which is classified as a 'cell death inhibitor', is upregulated in motor neurons[19]. The upregulated NF-κB may induce the overexpression of OPTN, and may also cause neuronal cell death[20]. Thus NF-κB is a major candidate target for treating this disease. Additionally OPTN plays an important role in the maintenance of the Golgi complex, in membrane trafficking, in exocytosis, through its interaction with myosin VI and Rab8 (ref. 13), and in post-Golgi trafficking to lysosomes dependent on the Rab8/OPTN/htt complex[21] (Supplementary Fig. 8). Interestingly, FUS/TLS has been reported to interact with myosin VI[22] as well as with myosin V[23]. Impairment of intracellular trafficking of the complex including OPTN and/or FUS/TLS may cause inclusions in this neurodegenerative disorder.

METHODS SUMMARY

Genotyping and extraction of candidate regions. The genotype of the GeneChip Human Mapping 500K Array Set (Affymetrix) was performed by AROS Applied Biotechnology. Computer analyses of the SNPs were performed by a homozygosity mapping algorithm accommodated to the whole-genome SNP scan data (Supplementary Information). To investigate the existence of a large insertion or deletion in this region, we analysed the copy number using Affymetrix Genotyping Console version 4.0 for the Affymetrix Mapping 500K data.

Full Methods and any associated references are available in the online version of the paper at www.nature.com/nature.

Received 17 August 2009; accepted 2 March 2010.
Published online 28 April 2010.

1. Leigh, P. N. in *Handbook of Clinical Neurology: Amyotrophic Lateral Sclerosis* Vol. 82 (eds Eisen, A. A. & Shaw, P. J.) 249–278 (Elsevier, 2007).
2. Rosen, D. R. *et al.* Mutations in Cu/Zn superoxide dismutase gene are associated with familial amyotrophic lateral sclerosis. *Nature* **362**, 59–62 (1993).
3. Greenway, M. J. *et al. ANG* mutations segregate with familial and 'sporadic' amyotrophic lateral sclerosis. *Nature Genet.* **38**, 411–413 (2006).
4. Sreedharan, J. *et al.* TDP-43 mutations in familial and sporadic amyotrophic lateral sclerosis. *Science* **319**, 1668–1672 (2008).
5. Kwiatkowski, T. J. *et al.* Mutations in the *FUS/TLS* gene on chromosome 16 cause familial amyotrophic lateral sclerosis. *Science* **323**, 1205–1208 (2009).
6. Vance, C. *et al.* Mutations in FUS, an RNA processing protein, cause familial amyotrophic lateral sclerosis type 6. *Science* **323**, 1208–1211 (2009).
7. Rezaie, T. *et al.* Adult-onset primary open-angle glaucoma caused by mutations in optineurin. *Science* **295**, 1077–1079 (2002).
8. Huqun, et a. l. Mutations in the SLC34A2 gene are associated with pulmonary alveolar microlithiasis. *Am. J. Respir. Crit. Care Med.* **175**, 263–268 (2007).
9. Li, Y., Kang, J. & Horwitz, M. S. Interaction of an adenovirus E3 14.7-kilodalton protein with a novel tumor necrosis factor alpha-inducible cellular protein containing leucine zipper domains. *Mol. Cell. Biol.* **18**, 1601–1610 (1998).
10. Schwamborn, K., Weil, R., Courtois, G., Whiteside, S. T. & Israël, A. Phorbol estersand cytokines regulate the expression of the NEMO-related protein, a molecule involved in a NF-κB-independent pathway. *J. Biol. Chem.* **275**, 22780–22789 (2000).
11. Wagner, S. *et al.* Ubiquitin binding mediates the NF-κB inhibitory potential of ABIN proteins. *Oncogene* **27**, 3739–3745 (2008).
12. Hattula, K. & Peränen, J. FIP-2, a coiled-coil protein, links huntingtin to Rab8 and modulates cellular morphogenesis. *Curr. Biol.* **10**, 1603–1606 (2000).
13. Sahlender, D. A. *et al.* Optineurin links myosin VI to the Golgi complex and is involved in Golgi organization and exocytosis. *J. Cell Biol.* **169**, 285–295 (2005).
14. Zhu, G., Wu, C. J. & Ashwell, J. D. Optineurin negatively regulates TNFα-induced NF-κB activation by competing with NEMO for ubiquitinated RIP. *Curr. Biol.* **17**, 1438–1443 (2007).
15. De Marco, N., Buono, M., Troise, F. & Diez-Roux, G. Optineurin increases cell survival and translocates to the nucleus in a Rab8-dependent manner upon an apoptotic stimulus. *J. Biol. Chem.* **281**, 16147–16156 (2006).
16. Chalasani, M. L., Balasubramanian, D. & Swarup, G. Focus on molecules: optineurin. *Exp. Eye Res.* **87**, 1–2 (2008).
17. Iwase, A. *et al.* The prevalence of primary open-angle glaucoma in Japanese: the Tajimi Study. *Ophthalmology* **111**, 1641–1648 (2004).
18. Mrowka, R., Blüthgen, N. & Fähling, M. Seed-based systematic discovery of specific transcription factor target genes. *FEBS J.* **275**, 3178–3192 (2008).
19. Jiang, Y. M. *et al.* Gene expression profile of spinal motor neurons in sporadic amyotrophic lateral sclerosis. *Ann. Neurol.* **57**, 236–251 (2005).
20. Pizzi, M. & Spano, P. Distinct roles of diverse nuclear factor-κB complexes in neuropathological mechanisms. *Eur. J. Pharmacol.* **545**, 22–28 (2006).
21. Toro, D. *et al.* Mutant huntingtin impairs post-Golgi trafficking to lysozomes by delocalizing optineurin/Rab8 complex from the Golgi apparatus. *Mol. Biol. Cell* **20**, 1478–1492 (2009).
22. Takarada, T. *et al.* A protein–protein interaction of stress-responsive myosin VI endowed to inhibit neural progenitor self-replication with RNA binding protein, TLS, in murine hippocampus. *J. Neurochem.* **110**, 1457–1468 (2009).
23. Yoshimura, A. *et al.* Myosin-Va facilitates the accumulation of mRNA/protein complex in dendritic spines. *Curr. Biol.* **16**, 2345–2351 (2006).

Supplementary Information is linked to the online version of the paper at www.nature.com/nature.

Acknowledgements This work was supported in part by grants-in-aid from the Ministry of Education, Science, and Culture of Japan, by a grant from the Smoking Research Foundation to H. Kawakami, and by the Japan Science and Technology Agency, Core Research for Evolutional Science & Technology to T.T. We thank E. Nakajima for technical support, K. Nakayama, H. W. Shin, M. Omi and H. Nakamura for conducting some of the experiments, and T. Miki and K. Noda for providing some DNA samples and clinical information. This paper is dedicated to the patients and families who contributed to this project.

Author Contributions H. Kawakami designed and supervised the study. H.Mo. and K.H. extracted candidate genes. H.Ma. and M.K. performed sequencing analysis. H.Ma., H.Mo., Y.W., T.T., S.M., H. Kawakami and H.S. conducted molecular biological analysis. H.I., Y.K., H. Ku., H. Kato, K.O. and A.H. performed pathological analysis and provided pathological samples. Y.I., H.N., R.K., O.K., N.M., K.A., A.K., T.H, T.K., M.A., N.S. and K.K. collected clinical information and samples. H. Kawakami, H.Ma., H.I. and K.H. wrote the paper.

Author Information Reprints and permissions information is available at www.nature.com/reprints. The authors declare no competing financial interests. Correspondence and requests for materials should be addressed to H. Kawakami (hkawakam@hiroshima-u.ac.jp).

METHODS

Ethical considerations. The study was approved by the institutional review boards of the participating institutions. All examinations were performed after having obtained informed consent from all subjects or their families.

Subjects. Neurologists performed the clinical diagnosis. The mean age at onset of subjects with ALS was 59.9 years (range 10–85 years, including 14 cases confirmed by autopsy). The possibility of mutation of SOD1 was excluded.

Screening for the mutation of *OPTN*. A list of PCR primer pairs used to amplify individual *OPTN* in the regulatory regions (~1,000 bases upstream from transcription start sites), non-coding exons, coding exons and the surrounding sequences (50–100 bases) of the exons or intron 4 and 5 is provided in Supplementary Table 4. Deletion of Exon 5 was checked by using exon 4 forward and intron 5 reverse primer pairs. Direct sequence of the joining part was performed by using intron 4-2 forward primer or intron 5-6 reverse primer. Screening for the c.1502C>T mutation was performed by analysing restriction-fragment length polymorphism or direct sequencing on 781 healthy control subjects (mean age 62.3 years; range 30–100 years). Exon 12 was amplified and then restricted with MseI, and thereafter the products were electrophoresed in 2% agarose gel. The wild type was digested into 204-, 106-, 14- and 12-bp fragments, and the mutant type (204 bp) into 169 + 35-bp fragments. The c.1743A>G mutation was determined by direct sequencing. In the Affymetrix Mapping 500K, there were 11 SNPs in the *OPTN* gene. However, there are no SNP markers between exon 2 and exon 12 of *OPTN*, and additional quantitative PCR analysis of all exons of the *OPTN* gene was performed.

Luciferase assay. We investigated the activity of NF-κB by using the luciferase assay. Four types of complementary DNA (cDNA) from OPTN were inserted into separate pDNR (Clontech). These were wild (IMAGE clone 3831267), Q398X (recessive), E478G (dominant) and E50K (which causes glaucoma) types. pDNR vector was used as mock. NSC-34 cells were co-transfected with NF-κB reporter ($(Igk)_3$ conaluc plasmid) (a gift from S. Yamaoka) and pDNR-OPTN by using Lipofectamine 2000 (Invitrogen). Luciferase activity was measured 5 h after either PBS or TNF-α (10 ng ml^{-1}, R&D) stimulation by using a Dual-Luciferase Reporter Assay System (Promega). Consistent results were obtained by conducting three independent experiments.

Localization of OPTN. We investigated the localization of OPTN by using a 3×Flag tag. This was inserted into pcDNA3 (Invitrogen), and three types of OPTN cDNA (wild, E478G, E50K) were inserted after the 3×Flag tag. These plasmids were used to transfect NSC-34 cells with the aid of Lipofectamine 2000 (Invitrogen). GM130 (BD Transduction Laboratories) was used as a marker of the Golgi apparatus.

Immunofluorescence microscopy. Cells were grown on glass-bottomed glass dishes (Matsunami) coated with poly-L-lysine and laminin (Sigma Aldrich) and transfected by Lipofectamine 2000 (Invitrogen) according to the manufacturer's protocol; 24–48 h after transfection, the cells were fixed, blocked with normal serum and incubated with primary antibody at 4 °C overnight. Confocal images were acquired with an Olympus FV300 by using a ×100 oil immersion lens with a sequential-acquisition setting at a resolution of 512 pixels × 512 pixels with threefold magnification. Each cellular picture was generated by combining multiple optical images (10–15 slices, *z*-spacing of 0.2 μm) spanning 2–3 μm along the *z*-axis. Subcellular localization of Flag-tagged optineurin was verified by at least three independent experiments. More than 100 cells were photographed for each optineurin construct. The following antibodies were used: mouse monoclonal anti-GM130 (BD Transduction Laboratories, 1:1,000) and affinity-purified rabbit polyclonal anti-Flag (Sigma, 1:1,000).

Western blotting. We investigated the expression of OPTN by western blotting. Cell lysates were prepared from Epstein-Barr-virus immortalized B lymphocytes from subject 3, her brother and mother, and subject 4 by using standard protocols. Polyclonal antibodies recognizing the carboxy (C)-terminal part of OPTN (Cayman Chemical) and anti-rabbit IgG-HRP antibody (R&D Systems) were used. For the internal control, we used glyceraldehyde-3-phosphate dehydrogenase polyclonal antibody (IMGENEX).

Quantitative PCR with reverse transcription. Quantitative PCR with reverse transcription was performed by using THUNDERBIRD SYBR qPCR Mix (TOYOBO) and ABI 7900HT Fast Real Time PCR system (Applied Biosystems). Epstein-Barr-virus immortalized B lymphocytes were treated with cycloheximide (Sigma, 100 μg ml^{-1}) for 2 h before RNA extraction.

Immunohistochemistry of mouse nervous tissue. Several antibodies were tested for their use in detecting mouse OPTN in tissue sections (data not shown). Among them, rabbit polyclonal antibodies raised against various peptides of human/mouse OPTN origin gave consistent and reasonable results. One such antibody was OPTN-C raised against the C-terminal part of OPTN, which is identical between human and mouse (amino acids 575–591; Cayman Chemical). Immunohistochemistry was performed on adult DBA/2 mouse. Mice were transcardially fixed with 4% paraformaldehyde in PBS, post-fixed in the same fixative overnight, and then dehydrated in 30% sucrose in PBS overnight. Frozen sections were obtained by using a cryostat and mounted onto 3-triethoxysilylpropylamine (TESPA)-coated glass slides. After air-drying, the slides were washed in PBS and blocked for 2 h at room temperature in 5% BSA/0.3% Triton X-100 containing PBS. The sections were then incubated overnight at 4 °C with primary antibodies against OPTN diluted in 1% BSA/1% normal goat serum/0.3% Triton X-100/PBS. After several washes in PBS, Alexa-594-conjugated secondary antibody (Invitrogen) in PBS was applied. Pictures were taken with a camera attached to a fluorescence microscope (BIOREVO BZ-9000; Keyence).

Histochemistry. Post-mortem material from one of the OPTN mutant cases (subject 5) was available. Sections (6 μm) of formalin-fixed, paraffin-embedded spinal cord were examined with Klüver–Barrera and haematoxylin and eosin staining. Some sections stained with haematoxylin and eosin were photographed, decolourized and immunostained with OPTN-C (mouse monoclonal, 1:50,000) or OPTN-I (rabbit polyclonal, Cayman Chemical, 1:400). In addition, lumbar spinal cord tissue was obtained from clinically and neuropathologically proven cases of SALS (seven cases) and familial ALS with the A4V *SOD1* mutation (FALS, three cases). Six age-matched normal individuals served as controls. After confirmation of complete removal of the OPTN antibody, we immunostained the same sections with the anti-ubiquitin antibodies (mouse monoclonal, Santa Cruz Biotechnology, 1:400; rabbit polyclonal, Sigma, 1:600), anti-TDP-43 antibodies (mouse monoclonal, Abnova, 1:1,000; rabbit polyclonal, Proteintech Group, 1:4,000) or anti-SOD1 antibodies (mouse monoclonal, Lab Vision Corporation, 1:50; rabbit polyclonal, Stressgen Biotechnologies, 1:2,000).

doi: 10.1038/nature08971

Supplementary Table 2. Numbers of subjects examined for variation in *OPTN*

Journal	glaucoma	control
Japanese		
Hum. Genet. **113**, 276 (2003)	313	196
Am. J. Oph. **136**, 904 (2003)	247	89
Inv. Oph. Vis. Sci. **45**, 4359 (2004)	411	218
J. Glaucoma **13**, 299 (2004)	154	100
Japanese total (1728)	1125	603
Non-Japanese		
Science **295**, 1077 (2002)	52	270
Hum. Genet. **112**, 600 (2003)	48	48
Mol. Vision **9**, 217 (2003)	217	90
Am. J. Oph. **136**, 904 (2003)	801	162
Arch. Ophthalmol. **121**, 1181 (2003)	86	80
Inv. Oph. Vis. Sci. **45**, 3122 (2004)	89	165
Clin. Exp.Oph. **32**, 518 (2004)	27	94
Mol. Vision **11**, 284 (2005)	112	100
Mol. Vision **11**, 625 (2005)	400	281
Mol. Vision **11**, 792 (2005)	200	200
Mol. Vision **12**, 816 (2006)	100	100
J. Glaucoma **15**, 358 (2006)	67	100
Mol. Vision **13**, 151 (2007)	263	371
Mol. Vision **13**, 862 (2007)	150	98
Mol. Vision **14**, 487 (2008)	51	51
Mol. Vision **14**, 2367 (2008)	140	130
Non-Japanese total (5143)	2803	2340

Total: 6871

Supplementary Table 4. PCR primer pairs for *OPTN*

Location	Forward primer	Reverse primer
Promoter 8	cagcctctagcctcatctgc	cgccctctcctggtatctc
Promoter 7	ggcagggttgagagtcagg	atgggagggagggaagga
Promoter 6	gcatctgccttttttcctgtt	aggctcggctattcttgttg
Promoter 5	tcgctcctaccttgtcatcc	gaggcctccatctgtgtttt
Promoter 4	agcaaaaacgagtggaaagc	tgtgacggcgttaatcaaaa
Promoter 3	gcctggcattctcctctttc	caccctgcccattccata
Promoter 2	gtgacgccttagagcagtcc	gggtgcctagggctgatg
Promoter 1	gtcgggtggggtatggaat	gtgccgcctggagagaact
Exon 1	gggtggggtatggaatgg	gcgggtaccgttttcagg
Exon 2	tctatgtccacatggatgcc	tgcaaatcttcaaattcaaatctc
Exon 3	acacacacatgcacacatgc	tgcagaagttcctgtggaaa
Exon 4a	acacacacatgcacacatgc	taaatcctgtgcttccccac
Exon 5	ttcagagccatgtggtcaag	tccagactgaaccatgaaagg
Exon 6	ggtgcccagccttagtttg	ttgtttcatctttccagggg
Exon 7	tgtgttaaatcccttgcatttc	aacatttgacctccggtgac
Exon 8	accttccctaggaagcatgg	gacagtgagtgctgtttggg
Exon 9	aacccctgatcctttatccc	aaagcaaataacccatcacaag
Exon 10	gttggattgattcaccagcc	tttcaaaggaggataaaattgc
Exon 11	aaaccctacagccctaaaattc	tgctaggactccttcagataagtg
Exon 12	cgtggggtgataaaggtagg	ggaaaacaaccctttgaaaccag
Exon 13	cggccagagctgataattaaa	tctaaacaccattgctttccaa
Exon 14	gggctattgaaggatacagcac	gcgcgaacacagctattc
Exon 15	tgaaccttggcagtgtagtttg	gtaatgagactgacgggtgc
Exon 16	gggaagcaggtatcacttgg	caggtacctttcttctccttcc
Exon 4	cgagaaccaccagctgaaag	tgctacttccttgagatacacaca
Intron 4-2	ggcaaggctaaatctgttctg	tccccagtagctaggaccag
Intron 4-3	gcaagatggcaagacctga	cttgagataccaggatgctttc
Intron 4-4	aaggaagaaaggctgctatgg	gcgggatgaacatcatttcta
Intron 4-5	gcggtacccaaatccacttt	gcttctgcaggaggttcaga

Intron 5-1	gggaaatcagaaaggtcatctg	cggtcaaagctttacaaatttcttt
Intron 5-2	tgccctattaagggtcatgg	tgagagaacagacaaggtcaaca
Intron 5-3	gcctctgcctagaaccaaca	ttgtgtcattactatcatctttgaca
Intron 5-4	gcattgccacagatgaaaag	ggcaacagtggactcataagc
Intron 5-5	aggaaaagggcaggaggtt	accctagcctcccaaagc
Intron 5-6	tcaaaataaatcgtgggctagg	tcagcttactgcatcctcca
Intron 5	tggtagtgcgtgcctgtagt	taaggacctggccatgagac
Intron 5-8	aacttccttgtcagtaggtgtgg	acacagtgaaaccccgtctc
Intron 5-9	gtggcataatctcggctca	gactgccaagaccctgtctc
Intron 5-10	gatggtctccatcttcctga	cttgaggccaggattttga
Intron 5-11	tgtaaagatgggggtcttgc	ctgagctggtccttttcctg

Supplementary Figure 1. Homozygosity mapping.

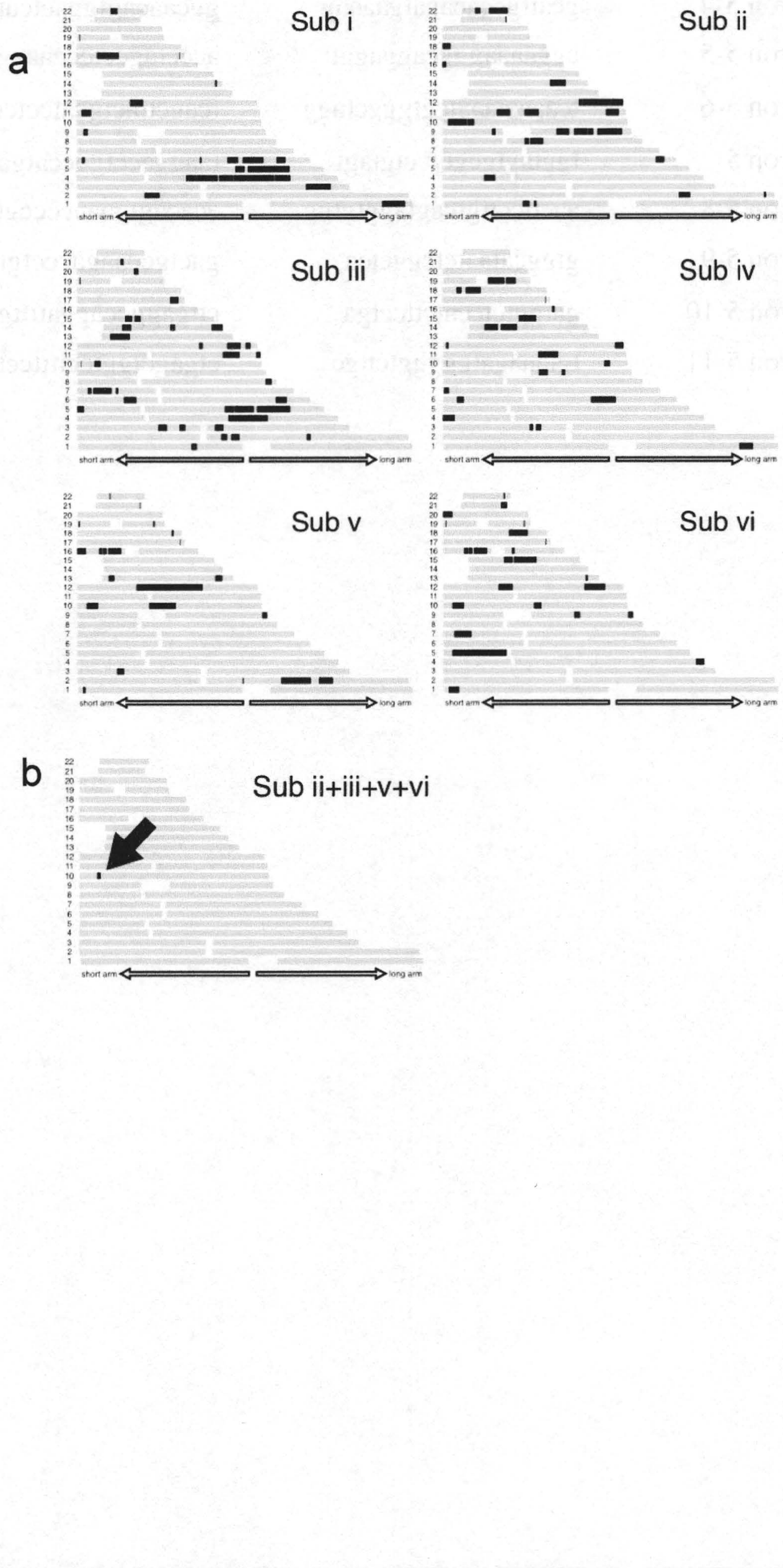

c

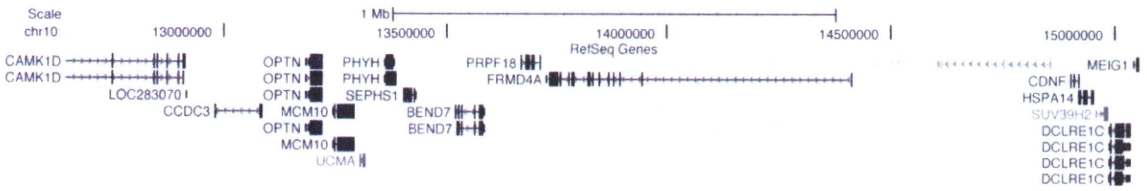

d

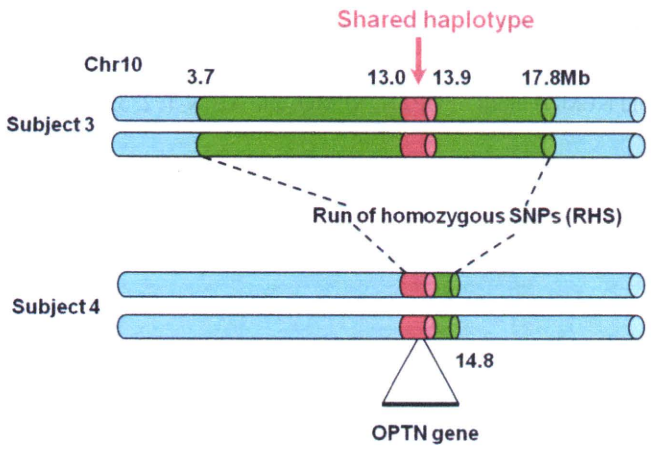

Supplementary Figure 1. Homozygosity mapping. a, Runs of SNPs (RHS) for each subject (Sub) is shown on the background indicating each chromosome. Sub ii, Subject 3 in Family 2; Sub v, Subject 1 in Family 1; and Sub vi, Subject 2 in Family 1. b, The overlap of RHSs for 4 individuals (ii, iii, v and vi). The arrow indicates an RHS located on chromosome 10, which contains the *OPTN* gene. c, Genes in the candidate region of chromosome 10. d, Schematic shared haplotype of Subject 3 and 4 in chromosome 10.

a

species	468-488
Homo sapiens	MEVYCSDFHAERAAREKIHEE
Pan troglodytes	MEVYCSDFHAERAAREKIHEE
Bos taurus	MEVYCSDFHAERAAREKIHEE
Felis catus	MEVYCSDFHAERAAREKIHEE
Mus musculus	MEVYCSDFHAERAAREKIHEE
Monodelphis domestica	MEVYCSDFHAERAAREKIHEE
Gallus gallus	MEVYCSDFHAERAAREKIHEE
Xenopus tropicalis	IDVYCADFHAERSARENIHQE
Oryzias latipes	AEVYSSDFYAERAAREKLHEE
Drosophila melanogaster	NDIYRRDFEMERADREKNAGE

b

protein	468-488
OPTN	MEVYCS DFHAER AAREKIHEE
NEMO	ADIYKA DFQAER QAREKLAEK
ABIN-1	VKIFEE DFQRER SDRERMNEE
ABIN-2	ILAYKD DFMSER ADRERAQSR
ABIN-3	VQIYEE DFKKER SDRERLNQE
	DFxxER motif
Consensus	DF ER RE

Supplementary Fig2. Sequence alignment. a, OPTNs in different species. b, UBAN (ubiquitin binding in ABIN and NEMO) motif of OPTN, NEMO, and ABIN-1, 2, 3. The box shows the DFxxER motif.

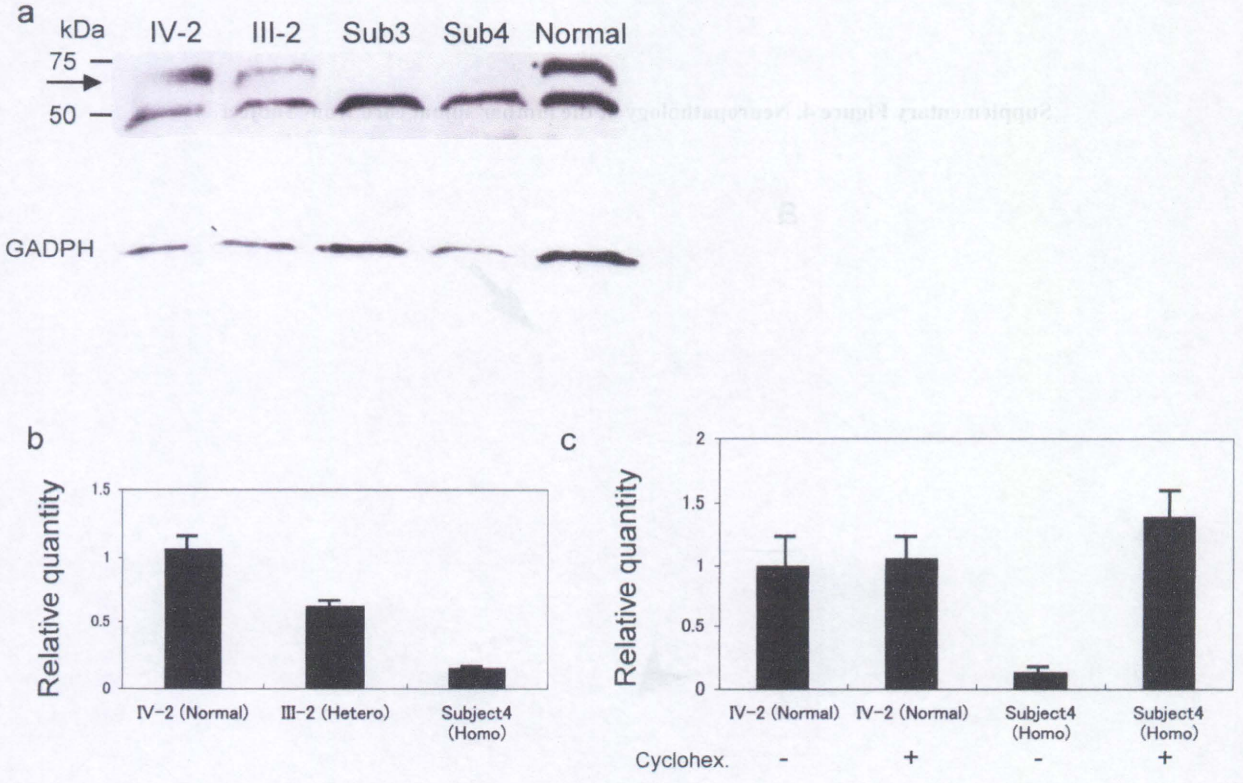

Supplementary Figure 3. Western blotting (a) and quantitative reverse transcription-PCR(b, c). Western blotting using polyclonal antibody against the C-terminal part of OPTN was carried out (a). The 74-kDa band is absent in the subjects. GADPH expression is shown below as a protein loading control. (b) Quantitative reverse transcription-PCR revealed that the products were diminished when nonsense c.1502C>T mutation was present. (c) Cycloheximide recovered this decrease.

Supplementary Figure 4. Neuropathology of the lumbar spinal cord from Subject

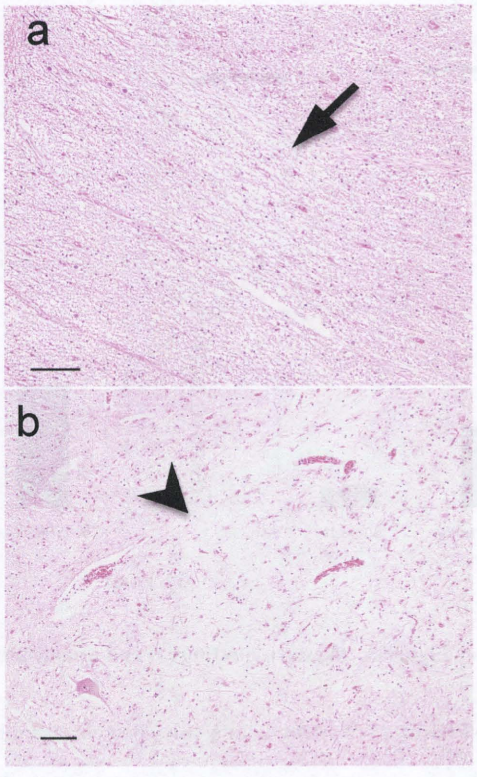

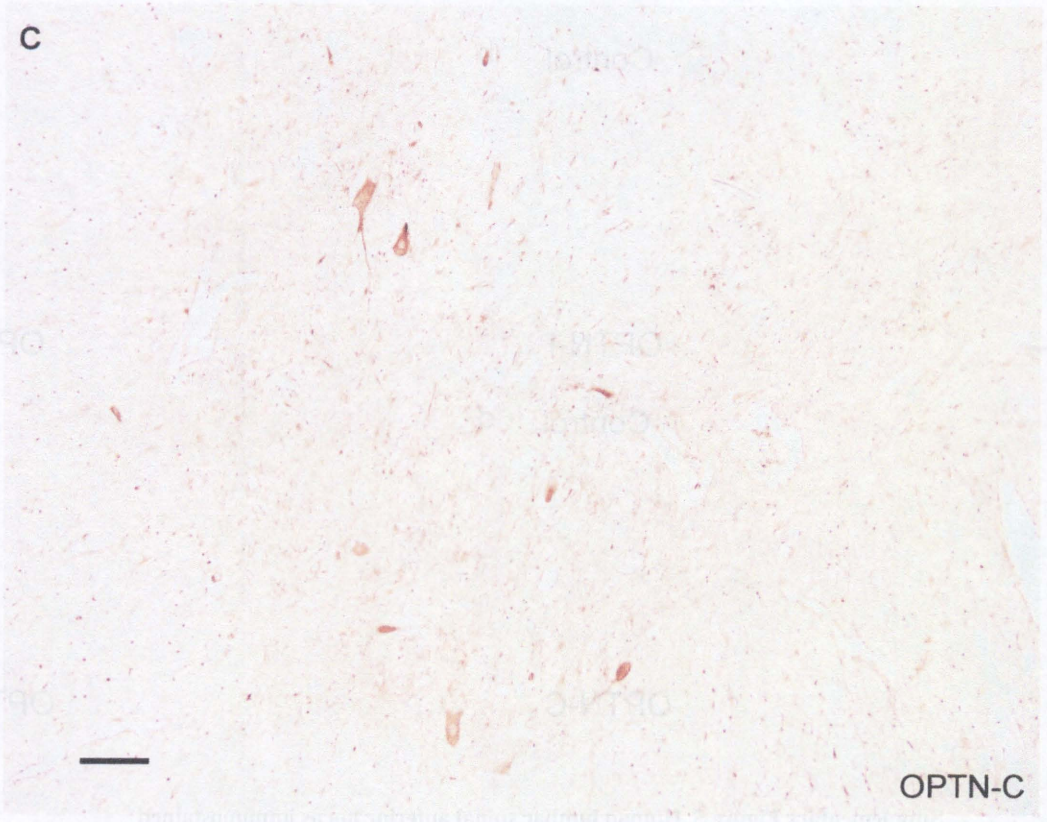

Supplementary Figure 4. Neuropathology of the lumbar spinal cord from Subject 5. H&E stainings (a, b) show loss of myelin from the corticospinal tract (arrow in a) and loss of motor neurons from the anterior horn (arrowhead in b).

OPTN-immunohistochemistry of the lumbar anterior horn (c) shows that the cytoplasm of the residual motor neurons is increased in volume and that the intertwined neurites are evidently reactive to the antibody.

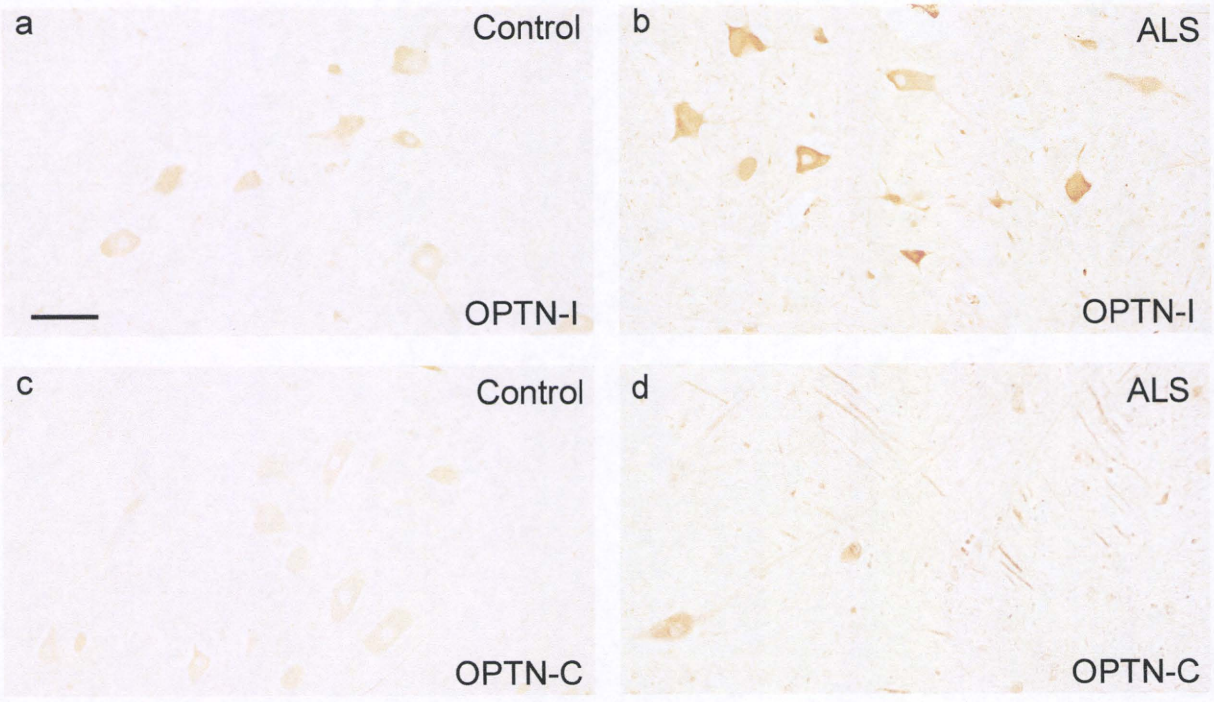

Supplementary Figure 5. Human lumbar spinal anterior horns immunostained with the anti-OPTN antibody. Immunoreactivities for both OPTN-I and OPTN-C are increased diffusely in the cytoplasm of anterior horn cells of the SALS patients (b, d), when compared with those in the control subjects (a, c). Numerous neurites immunopositive for OPTN are evident in the SALS cases (b, d). Scale bar = 100 μm.

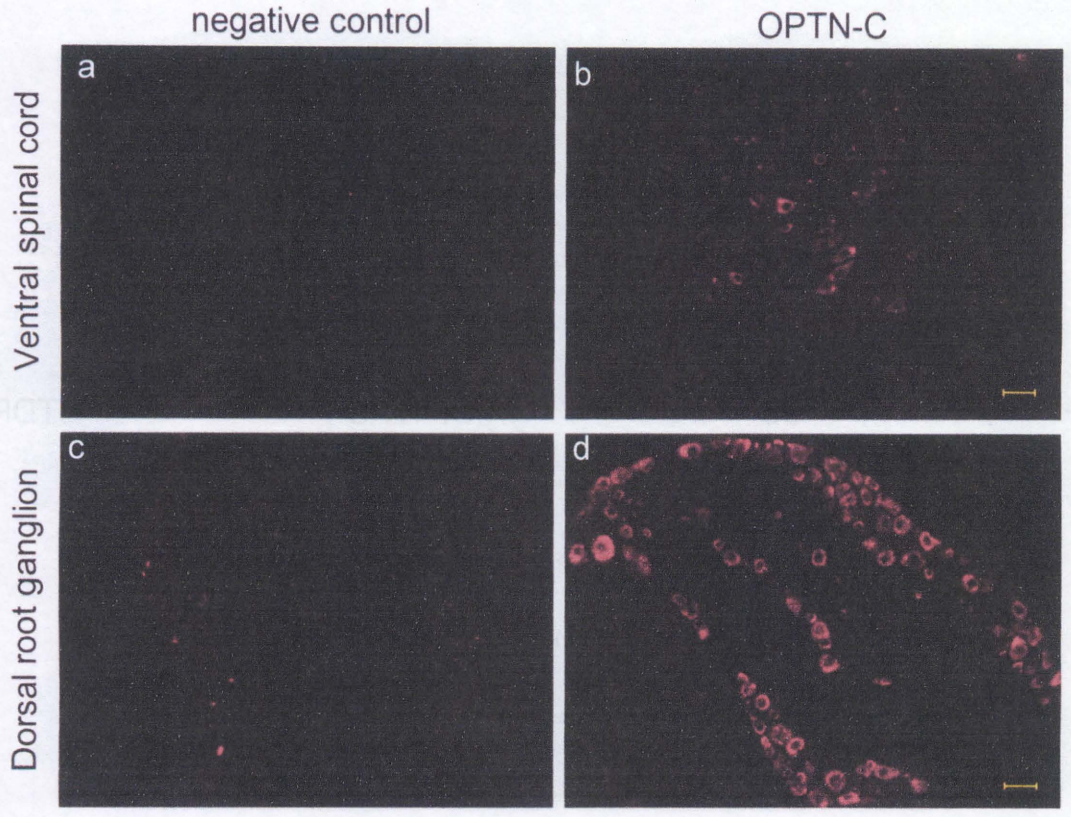

Supplementary Figure 6. OPTN expression in the mouse spinal cord and dorsal root ganglia. Ventral spinal cord (motor neuron-containing region; a and b) and dorsal root ganglia (DRG; c and d) at the lumbar level. The OPTN-C antibody gave a clearly discernible staining pattern in both tissues. Low-level staining (b), but clearly over the background level of the primary antibody-negative control (a), was observed in the motor neurons of the spinal cord ventral horns. An equally exposed film gave an image depicting strong fluorescet signals in the cytosol of the primary sensory neurons of the DRGs (d). Scale bars = 50 μm.

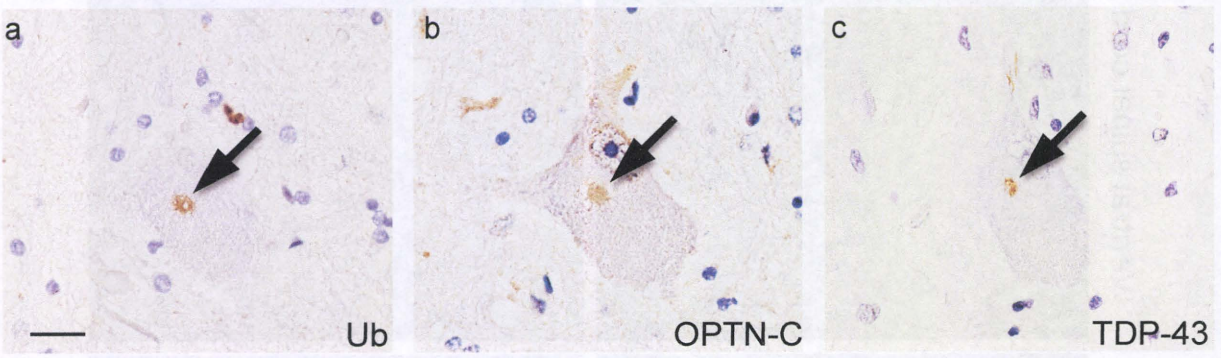

Supplementary Figure 7. Serial sections of the lumbar spinal cord from a SALS patient, immunostained for ubiquitin(a), OPTN(b), and TDP-43(c). Note the same cytoplasmic round hyaline inclusion of the anterior horn cell is labeled with all the antibodies (arrows). Scale bar = 20μm.

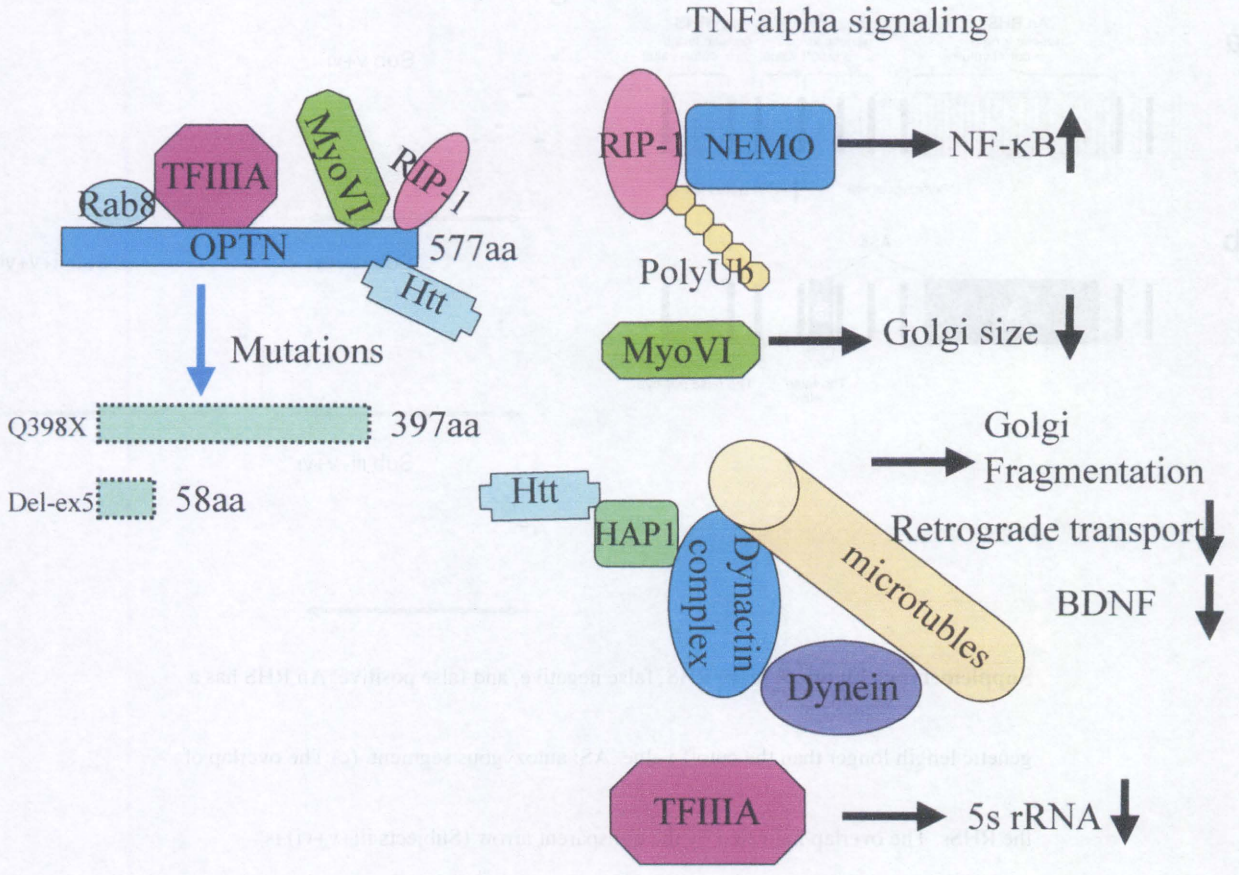

Supplementary Figure 8. Pathomechanism of truncated OPTN.

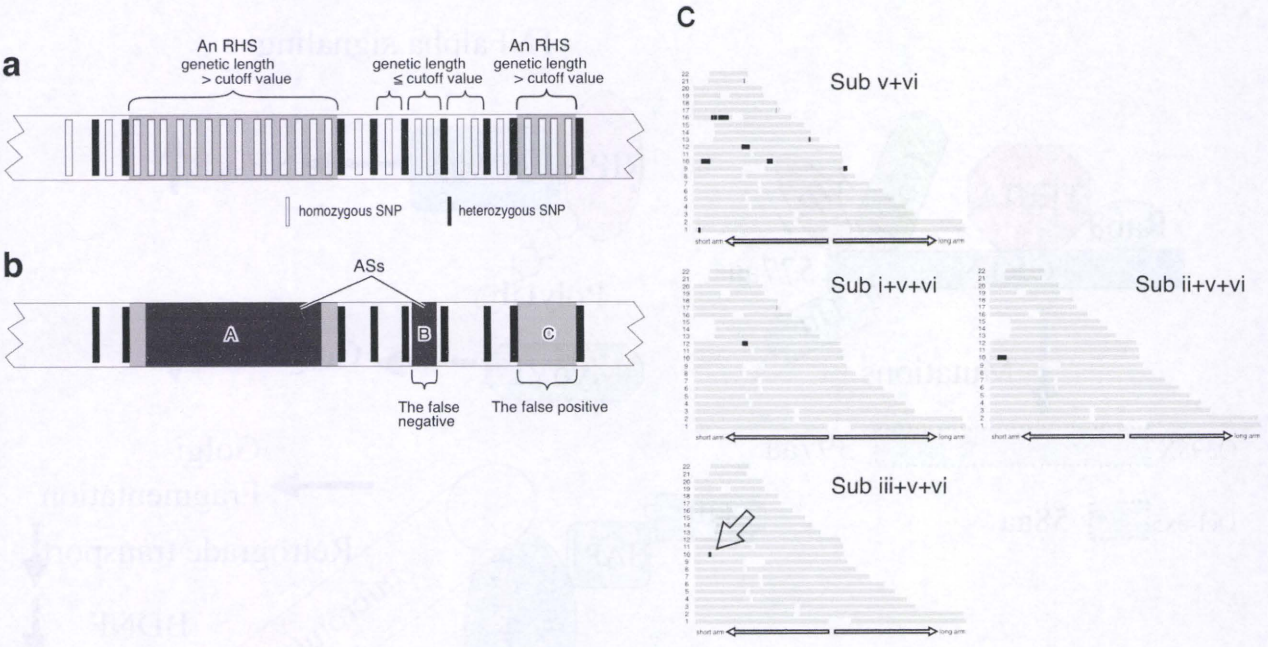

Supplementary Figure 9. (a, b) RHS, false negative, and false positive. An RHS has a genetic length longer than the cutoff value. AS: autozygous segment. (c) The overlap of the RHSs. The overlap indicated by the transparent arrow (Subjects iii+v+vi) is contained in the overlap for Subjects ii+v+vi.

Patient Information

Subject 1 (Family 1, V-1) developed onset with muscle weakness of her left upper limb at 33 years of age. Two years later, she could walk by herself; but dysphagia appeared, and she was endotracheally intubated. She became bedridden at the age of 34, and died at age of 57. Subject 2 (Family 1, V-2) showed onset with muscle weakness of his left upper limb at 36 years of age. One year later, he showed dysphagia and dysarthria, and developed fasciculation of the tongue. He showed narcosis, and endotracheal intubation was done. He became bedridden at the age of 37. He could not eat at age 38, and could not speak at age 41. He died at the age of 55. Subject 3 (Family2, IV-1) developed onset with dysarthria at 52 years of age. Muscle weakness of left upper and lower limbs occurred 2 years later. Her deep tendon reflex was exaggerated, but there was no pathological reflex. She still respired by herself after 8 years from the onset. Subject 4 (Family 3) is a sporadic case with onset, manifesting as right-limb muscle weakness at 44 years of age. One year later, she could not open a screw cap. Her deep tendon reflex was normal, and no pathological reflex was noted. Fasciculation was observed at her tongue and right upper limb. She still respired by herself after 3.5 years from onset. Subject 5 (Family 4, II-2) showed onset with muscle